HHS Public Access

Author manuscript

J Colloid Interface Sci. Author manuscript; available in PMC 2021 October 01.

Published in final edited form as:

J Colloid Interface Sci. 2020 October 01; 577: 406–418. doi:10.1016/j.jcis.2020.05.088.

Platelet-like particles improve fibrin network properties in a hemophilic model of provisional matrix structural defects

Seema Nandi[1,2], **Laura Sommerville**[3], **Kimberly Nellenbach**[1,2], **Emily Mihalko**[1,2], **Mary Erb**[1], **Donald O. Freytes**[1,2], **Maureane Hoffman**[3], **Dougald Monroe**[4], **Ashley C. Brown**[*,1,2]

[1]Joint Department of Biomedical Engineering, University of North Carolina at Chapel Hill and North Carolina State University, Raleigh, NC

[2]Comparative Medicine Institute, North Carolina State University, Raleigh, NC

[3]Department of Pathology, Duke University, Durham, NC

[4]Division of Hematology/Oncology, University of North Carolina at Chapel Hill, Chapel Hill, NC

Abstract

Following injury, a fibrin-rich provisional matrix is formed to stem blood loss and provide a scaffold for infiltrating cells, which rebuild the damaged tissue. Defects in fibrin network formation contribute to impaired healing outcomes, as evidenced in hemophilia. Platelet-fibrin interactions greatly influence fibrin network structure via clot contraction, which increases fibrin density over time. Previously developed hemostatic platelet-like particles (PLPs) are capable of mimicking platelet functions including binding to fibrin fibers, augmenting clotting, and inducing clot retraction. In this study, we aimed to apply PLPs within a plasma-based *in vitro* hemophilia B model of deficient fibrin network structure to determine the ability of PLPs to improve fibrin structure and wound healing responses within hemophilia-like abnormal fibrin network formation. PLP impact on structurally deficient clot networks was assessed via confocal microscopy, a micropost deflection model, atomic force microscopy and an *in vitro* wound healing model of early cell migration within a provisional fibrin matrix. PLPs improved clot network density, force generation, and stiffness, and promoted fibroblast migration within an *in vitro* model of early wound healing under hemophilic conditions, indicating that PLPs could provide a biomimetic platform for improving wound healing events in disease conditions that cause deficient fibrin network formation.

Graphical Abstract

[*]**Correspondence:** Ashley C. Brown, PhD, Joint Department of Biomedical Engineering, University of North Carolina at Chapel Hill/ North Carolina State University, 1001 William Moore Dr., Biomedical Partnership Center 20081, Raleigh, NC 27607, aecarso2@ncsu.edu.

Author Contributions

Seema Nandi, Kimberly Nellenbach, Emily Mihalko, and Mary Erb performed experiments; Seema Nandi, Laura Sommerville, Emily Mihalko, Maureane Hoffman, Dougald Monroe, and Ashley C. Brown analyzed results; Seema Nandi made figures; Seema Nandi, Laura Sommerville, Donald O. Freytes, Maureane Hoffman, Dougald Monroe, and Ashley C. Brown designed the research; Seema Nandi and Ashley C. Brown wrote the paper.

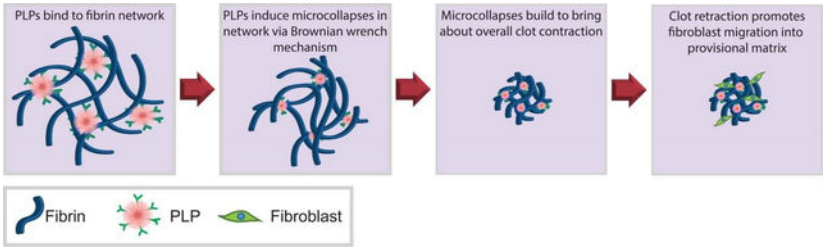

Keywords

fibrin; biomimetic; platelet; hemophilia; biomaterials

Introduction

Following injury, a fibrin-rich provisional matrix is formed that stems blood loss and provides a scaffold for infiltrating cells to rebuild the damaged tissue. Platelet-fibrin interactions greatly influence fibrin network structure, both through platelets' ability to induce thrombin generation and through biophysical means such as clot retraction [1, 2]. Activated platelets promote the formation of a fibrin network via thrombin generation on the platelet surface, which catalyzes the conversion of soluble fibrinogen into an insoluble network of fibrin fibers. Platelets bind to fibrin via $\alpha_{IIB}\beta_3$ integrins to form a platelet-fibrin "plug" capable of stemming bleeding and achieving hemostasis [3, 4]. Following clot formation, platelets utilize actin-myosin machinery to contract the fibrin network in a process known as clot retraction, increasing fibrin density, stiffness, and stability [5–7]. The structural properties of the fibrin network influence the ability of the fibrin network to act as a provisional matrix supporting cellular infiltration, first by macrophages and then by fibroblasts and keratinocytes. Infiltrating fibroblasts deposit new extracellular matrix, thus facilitating tissue repair and long-term tissue remodeling [5, 6, 8, 9]. A fibrin network that is extremely porous, soft, and highly susceptible to fibrinolysis cannot properly support cellular infiltration, and, therefore, healing is impeded.

In cases of traumatic injury or disease, fibrin structural defects can arise due to a loss or dysfunction of platelets, coagulation factors or other blood components. When this occurs, fibrin formation and subsequent clot retraction processes are impaired, resulting in uncontrolled or recurrent bleeding and dysfunctional wound healing. Such fibrin defects can have severe consequences: exsanguination due to insufficient clot formation and the resultant uncontrolled bleeding is the leading cause of death for both men and women under the age of 45 [10]. Additionally, recurrent bleeding that arises as a result of disease conditions that impair normal fibrin network formation, such as hemophilia, can result in debilitating joint injuries, impaired mobility [11] and deficient healing responses [12].

Hemophilia is a particular example of a condition that arises as a result of a naturally occurring fibrin structural defect. In hemophilia, a lack of coagulation factor VIII or IX impairs robust fibrin network formation by preventing sufficient platelet-surface thrombin generation [3, 12]. This results in weak, easily disrupted fibrin networks with modified matrix properties, including thicker fibers and less dense structure [13, 14], that are

incapable of providing the hemostatic and provisional matrix functions that would normally be provided by a robust fibrin clot formed following an injury [12]. The defective fibrin formation seen in hemophilia is a model for the type of defect seen in other genetic diseases such as von Willebrand Disease or in patients taking oral anticoagulants [15–17]. In recent years, artificial blood cells made from synthetic materials have shown promise in recapitulating native blood cell functions for the treatment of various coagulopathies; artificial platelets, in particular, have been used in order to improve clotting and stem bleeding in *in vitro* and *in vivo* models of uncontrolled bleeding [2, 18–20]. Due to their ability to mimic native platelet functions in hemostasis, artificial platelet constructs are of particular interest in developing alternative treatments for bleeding disorders such as hemophilia.

In these studies, we investigate whether deficient fibrin matrix structures can be improved to recapitulate the mechanical and structural properties of a healthy fibrin matrix through the use of synthetic platelets that augment clot formation and actively modify fibrin matrices. These synthetic platelet-like particles, or PLPs, are colloidal micro-scale hydrogel particles that are designed to mimic key mechanical properties of native platelet bodies [20]. In particular, PLPs are capable of mimicking the fibrin-binding ability of native platelets, thereby promoting clot formation. Additionally, PLPs also mimic the clot retraction abilities of native platelets, thereby stabilizing the clot network and allowing it to facilitate downstream healing processes. Colloidal microparticles have been of significant interest in the areas of biomaterials and tissue engineering in recent years, with much emphasis being placed on the development of biocompatible and/or biodegradable materials that are capable of sensing and responding to changes in their biological environment in biomimetic or tunable manners [21, 22]. Colloidal micro- and nanoparticles are capable of influencing cellular responses via changes in their chemical composition, viscoelasticity, surface topography, charge, wettability, modulus, and other chemical and physical characteristics. These features allow for dynamic modulation of cellular adhesion, protein adsorption on particle surfaces, cellular proliferation and differentiation, and extracellular matrix properties in order to bring about desired cellular behaviors [21–24]. Several studies detailing the development of polymeric microparticles as a platform for developing synthetic biomimetic blood cells have been published over the past decade [18–20, 25–27]; techniques involving colloidal hydrogel microparticles in particular have shown that these particles are highly tunable and are able to achieve degrees of elasticity and softness that allow them to mimic desired mechanical properties, remain in circulation longer than conventional microparticles, and pass through pores smaller than their own dimensions [20, 25, 28]. These features permit these colloidal microparticle-based technologies to recapitulate key characteristics of native blood cells. Ultralow crosslinked poly(*N*-isopropylacrylamide) (pNIPAM) microgels (ULCs) are of additional interest for this application due to their low crosslinking density and their temperature- and pH-sensitivity [29], which has allowed them to be utilized in a range of biomedical applications including drug delivery, artificial tissue constructs, and sensors, among others [30]. pNIPAM ULCs are synthesized in the absence of any exogenous crosslinkers and have been shown to exhibit only a small degree (≤ 0.5%) of self-crosslinking primarily located within the core of the microgel, which occurs due to interchain transfer during the polymerization process [28, 30]. Furthermore, incorporation of

certain comonomers, such as acrylic acid, have been shown to increase particle size and decrease crosslinking density, increasing the deformability and softness of these pNIPAM ULCs [31].

In the studies described herein, we investigate the application of colloidal microscale synthetic PLPs, made by coupling pNIPAM ULCs to a fibrin-binding antibody [20], within a model of hemophilia B in order to augment clotting and improve fibroblast migration. Previous studies that have applied PLPs within fibrin clots have done so in simplified systems using purified fibrinogen; physiological conditions, however, are more complex, requiring validation of these effects within a more physiologically-relevant clotting model in order to evaluate PLP ability to improve clotting and healing outcomes within models of coagulopathies. We modeled a hemophilia-like fibrin structural defect by inhibiting coagulation factor IX through the application of an anti-factor IX (fIX) antibody, resulting in deficient fibrin network formation and decreased stiffness relative to clots formed from healthy plasma. This model closely mimics hemophilia B, which results from a lack of fIX that leads to deficient thrombin generation upon native platelet surfaces, giving our model physiological relevance. Although hemophilia B is less prevalent than hemophilia A in the general population, both bring about a defect in fibrin clot structure. Additionally, the antibodies required to inhibit fIX activity are well-characterized, and hemophilia B has been shown to be associated with defective fibrin formation *in vivo* [32]. In this work, we aimed to investigate the efficacy of applying hemostatic PLPs within a model of defective clot formation; the hemophilia B model applied in these studies thus served as a well-characterized model for the basis of the experiments described herein. Within this model, we then investigated the ability of an active matrix modifier (a synthetic platelet-mimetic particle) to improve the deficient fibrin matrix and compared this effect to the effect of healthy platelets. The application of a synthetic platelet mimic is advantageous over native platelets due to the limited supply and short shelf life of native platelets for transfusions. Our lab has previously developed PLPs that bind fibrin forming at sites of injury and exert strain upon the bound fibrin fibers to mechanically induce clot retraction in a manner reminiscent of native platelets [20, 33] (Figure 1). PLPs are created by coupling a fibrin-binding antibody to a highly deformable microgel body. The highly deformable microgel is capable of undergoing robust morphological changes which, in combination with the high fibrin affinity of the attached antibodies, facilitates their clot retraction feature. As PLPs bind fibrin fibers, they deform and spread extensively between the bound fibers. PLPs eventually return to a more energetically favorable spherical conformation, thereby exerting strain upon the bound fibers and inducing microcollapses in the clot network that sum to bring about bulk clot contraction in a Brownian wrench mechanism, as has been illustrated previously [20]. In this mechanism, as spread PLPs collapse to return to a more energetically favorable spherical conformation, pulling the bound fibers with them to create a local microcollapse in the network, fibrin fibers in nearby locations are brought closer together. This facilitates further PLP binding and microcollapse events to occur, thus propagating the microcollapses throughout the network and eventually generating bulk clot collapse. When applied within fibrin clots under healthy conditions, PLPs have been shown to contribute to secondary hemostasis. Additionally, after clot formation, PLPs generate forces within clot networks and increase clot density and stiffness, thus improving the overall structural and mechanical

properties of these clot matrices [33]. Additionally, in healthy conditions, incorporation of PLPs into clot matrices has been shown to enhance *in vitro* cell migration and *in vivo* wound healing [33], which occurs at least in part due to increased clot stiffness. These effects occur not only due to the fibrin-binding ability of the PLPs, but also, critically, due to the deformability of the pNIPAM ULC microgel body; indeed, past studies have demonstrated that less deformable particles coupled to a fibrin-binding motif do not result in the same degree of clot retraction as that seen in the presence of PLPs formed using highly deformable pNIPAM microgels [20]. This is likely due to the fact that the low crosslinking density in the pNIPAM ULC microgel allows the PLP to spread and collapse in a manner necessary to bring about clot retraction after binding to fibrin, whereas more rigid particles are not able to mechanically deform to the same extent and are thus unable to bring about this necessary clot retraction event [20, 34]. We hypothesized that when applied within a model of deficient fibrin formation (i.e. hemophilia), PLPs will bind existing fibrin fibers to facilitate and augment clot formation, resulting in improved clot network properties and cell migration within the clot matrix. This hypothesis was investigated via confocal microscopy evaluation of clot structure, micropost deflection models to determine PLP-generated forces within clot networks, atomic force microscopy nanoindentation to determine clot moduli, and *in vitro* assays to determine the effect of PLP-induced clot augmentation on overall fibroblast migration responses within a provisional clot matrix. The results of these studies indicate that, when applied within a hemophilia-like model of deficient fibrin structural formation, PLPs are able to improve clot density and stiffness and bring about increased fibroblast migration within an *in vitro* model of early wound healing.

Materials and Methods

Ultra-low crosslinked microgel (ULC) synthesis and characterization

Poly(*N*-isopropylacrylamide-*co*-acrylic acid) (pNIPAm-*co*-AAc) ULCs were synthesized in a precipitation polymerization reaction carried out under constant stirring at 450 rpm for a duration of 6 hours at 70 °C. NIPAm (Sigma-Aldrich, St. Louis, MO, USA, 97% purity) was dissolved in 100 mL ultrapure water in a three-necked reaction vessel (18.2 Ω, Milli-Q, Darmstadt, GER) and heated to 70 °C in a silicon oil bath while being purged with nitrogen. Upon reaching 70 °C, the monomer solution was allowed to equilibrate under nitrogen purging for one hour prior to initiation of the reaction. Acrylic acid (Sigma-Aldrich, 99% purity) was added to the monomer solution 10 minutes prior to initiation in order to achieve a final monomer concentration of 140 mM. The reaction was initiated using 1 mM ammonium persulfate (APS) (Sigma-Aldrich, 98% purity) and allowed to proceed for 6 hours. The monomer solution turned opaque following addition of the APS, allowing for visual confirmation of the reaction. After 6 hours, the reaction was cooled to room temperature overnight under constant stirring at 450 rpm and then filtered through glass wool. The filtered ULC suspension was purified via dialysis (MWCO: 1000 kD, Spectrum Laboratories, Rancho Dominguez, CA, USA) against ultrapure water for 3 days, then lyophilized and resuspended in ultrapure water prior to use in experiments.

ULC characterization was performed via dynamic light scattering (DLS) using a Malvern Zetasizer Nano S (Malvern Instruments, Worchestershire, UK) to determine the

hydrodynamic radii of the microgels. ULCs were resuspended in 10 mM HEPES buffer, pH 7.4; five measurements of at least 12 runs each were taken to determine average ULC hydrodynamic radii. Average hydrodynamic radius ± standard deviation is reported.

To confirm particle deformability and morphology, ULC spreading behavior was evaluated by depositing ULCs on a glass surface and determining height and spread area of the microgels using atomic force microscopy (AFM) on an Asylum Research MFP-3D Bio atomic force microscope (Asylum Research, Santa Barbara, CA, USA) operated in intermittent contact mode using silicon nitride cantilevers (k = 42 N ml, NanoWorld) [34]. Prior to ULC deposition, glass coverslips were prepared for AFM via submersion in a series of solutions (alconox, water, acetone, absolute ethanol, and absolute isopropyl alcohol) in an ultrasonic bath. Cleaned coverslips were dried overnight and ULCs were deposited onto the clean coverslips for AFM dry imaging. Height traces were determined using the AFM software (Igor Pro 15). Average height ± standard deviation is reported.

PLP synthesis

ULCs were coupled to an anti-fibrin fragment E antibody via EDC/NHS chemistry in order to create PLPs [33, 35]. 50 mg/ml 1-Ethyl-3-(3-dimethylaminopropyl) carbodiimide (EDC) (Fisher Scientific, Waltham, MA, USA) in ultrapure water and 5 mg/ml sulfo-*N*-hydroxysuccinimide (NHS) (Fisher Scientific) in ultrapure water were combined with 0.5 mg/ml ULCs in ultrapure water and incubated for 30 minutes. After 30 minutes of incubation, a sheep anti-human fibrin fragment E polyclonal IgG antibody (Affinity Biologicals, Ancaster, ON, CAN) was added to the ULC suspension at a 2:1 ratio of antibody:AAc content in the ULCs. AAc concentration was assumed from the synthesis conditions, in which AAc comprised 10% of the total monomer solution. After 3 hours of incubation with the antibody, PLPs were dialyzed (MWCO: 1000 kD, Spectrum Laboratories) against ultrapure water for 24 hours at 4°C. Dialysis buffer was changed 3 times over the course of 24 hours. Purified PLPs were lyophilized and stored at 4°C prior to resuspension in ultrapure water for use in experiments. PLPs were sterilized using UV light prior to all *in vitro* experiments.

Preparation of normal and hemophilia B-like platelet-poor plasma (PPP) and platelet-rich plasma (PRP)

Whole blood was collected into citrate tubes by venipuncture of healthy adult volunteers. Citrated blood was centrifuged at 2000 × g for 10 minutes to isolate platelet-poor plasma or 800 × g for 8 minutes to isolate platelet-rich plasma. Where indicated, plasma fIX activity was inhibited by addition of 2 mg/ml anti-human fIX antibody (Affinity Biologicals) to model hemophilia B-like PPP or PRP. Platelet-rich plasma was further prepared by diluting PRP obtained from whole blood with previously collected PPP to obtain normal and hemophilia B-like PRP with a platelet count of 1×10^5 platelets/μL, in order to minimize variations in clotting responses as a function of varied platelet count. Blood collection was performed under a protocol approved by the Institutional Review Boards of both the Durham Veterans Affairs and Duke University Medical Centers.

Evaluation of PLP thrombogenicity

Thrombogenicity of synthetic PLPs was evaluated using a plate-based fluorescence assay in which platelet-poor plasma was incubated with 3 pM tissue factor (Innovin, Dade Behring Gmbh, Marburg, GER), a fluorescent substrate that is cleaved by thrombin during the clotting cascade, and recalcified using 12 mM $CaCl_2$ to induce a thrombogenic reaction. Plasma and tissue factor were incubated with either lipids (0.2 μM – 10 μM) or PLPs (0 – 5 mg/ml) to determine the relative thrombogenicity of PLPs when applied across a range of therapeutic concentrations. Thrombin concentration was indirectly measured via fluorescence of the plasma + tissue factor + PLP/lipid mixture over 10 minutes following the addition of calcium. Samples were run in duplicate, and average curves are reported for each condition.

Formation of normal and hemophilic clots

Clots were formed from either normal (healthy) or hemophilia B-like PPP through recalcification. PPP was recalcified with 16.7 mM sterile filtered $CaCl_2$ (Fisher Scientific, ≥99% purity) and incorporated with 0.5 mg/ml PLPs. Control clots, formed in the absence of PLPs, were also formed via recalcification of either normal or hemophilia B-like plasma. For confocal microscopy and *in vitro* fibroblast migration assays, additional normal and hemophilia B-like PRP clots +/− functionalized PLPs (i.e. pNIPAM ULC microgels coupled to anti-fibrin antibodies) were created via recalcification as described for PPP clots. Additionally, confocal microscopy was performed on clots incorporated with 0.25, 0.5, or 1.0 mg/ml PLPs to evaluate the impact of PLP concentration on clot structure.

Determination of hemophilic clot structure in the presence of PLPs

Confocal microscopy was used to assess the fibrin network structure of 30 μL PPP clots formed as described above. A Zeiss Laser Scanning Microscope (LSM 710, Zeiss Inc., USA) was utilized at a magnification of 63X to image clot structure 16 hours after initial clot formation. In order to visualize fibers, 0.5 μL 2 mg/ml Alexa-fluor 488 labeled fibrinogen was added to clots prior to polymerization. Three random 5.06 μm z-stacks were imaged for each clot, with at least 3 clots imaged per condition. After imaging, z-stack projections were binarized using ImageJ image analysis software (National Institutes of Health, Bethesda, MD, USA) and a ratio of black pixels (fibrin fibers) to total pixels was determined to quantify clot network density. Mean network density ± standard deviation is reported for each group.

PPP clot structure was further evaluated using a JEOL 7600F cryogenic scanning electron microscope (cryoSEM) with a Gatan Alto cryo-transfer system. Clot samples were plunge-frozen in liquid nitrogen under high pressure, fractured, and etched for 7 minutes under vacuum. Etched samples were gold sputter-coated prior to imaging, and images were analyzed using the ImageJ plugin DiameterJ, which allows for structural analysis of fibrillar network images [36]. A minimum of three random images were taken per clot, with three clots imaged per group. Percent porosity ± standard deviation and intersection density ± standard deviation are reported for each group.

Evaluation of PLP-mediated force generation within hemophilic clot matrices

Force generated by PLPs within a fibrin network was determined by modifying an established micropost deflection technique [37–39] as described previously [33]. Microposts spaced at a 2 mm post center to post center distance were fabricated using Dow Corning Sylgard 184 polydimethylsiloxane (PDMS) (Krayden, Denver, CO, USA) poured into an aluminum mold machined by Xometry (Gaithersburg, MD, USA) [33] and cured for 2 hours at 90 °C. Posts had a diameter of 200 μm and a length (height) of 1 mm. Each post fabrication resulted in PDMS wells containing 16 independent sets of microposts, allowing up to 16 sets of measurements to be taken per experiment. Images were taken of each set of microposts after curing, and then microposts were seeded with normal or hemophilia B-like clots in the presence or absence of PLPs. Images were taken again following overnight clot polymerization. Post centers were determined in ImageJ using the known post geometry, and center-to-center distance for each set of posts was measured using images taken both before and after clot seeding. Changes in center-to-center distance were calculated, and the forces generated within the clot matrix, F, were determined based upon the distance of post deflection, δ, using Hooke's law:

$$F = k\delta$$

The spring constant k is calculated based upon the micropost geometry and elastic modulus using the formula

$$k = \frac{3\pi E D^4}{64 L^3}$$

where E represents the elastic modulus of the posts, D represents the diameter of the posts, and L represents the length of the posts. Based upon this calculation, the spring constant k was determined to have a value of 7.5 N/m; thus, force generation within the clot matrix for any given set of posts could be calculated from the formula

$$F = 7.5\delta$$

Three independent experiments were conducted, with 3–6 sets of microposts measured per condition for each experiment. Sets of microposts in which any post boundaries were not fully visible or in which any posts had broken during the process of removing the PDMS from the mold were not used for obtaining distance measurements. Modulus values were determined from the literature [40]. In order to control for potential variability in PDMS modulus due to efficiency of the curing process, all experimental and control group microposts for each experiment were formed from the same batch of PDMS and cured concurrently in the same location and for identical lengths of time. Approximate force generated ± standard deviation is reported for each group.

Evaluation of hemophilic clot stiffness in the presence of PLPs

Clot stiffness was evaluated via an Asylum MFP 3D Bio AFM operated in contact force mode using silicon nitride cantilevers (Nanoandmore, Watsonville, CA, USA) with a particle diameter of 1.98 μm. Clot stiffness was evaluated 16 hours after initial clot formation. AFM software Igor Pro 15 was used to determine the spring constant of each cantilever prior to force map collection. Each force map was fit by applying the Hertz model (using assumptions of a spherical tip geometry and a Poisson's ratio of 0.33) to the linear region of the force curve in order to determine the elastic modulus of the clot at each location measured. 3–4 random 10 μm × 10 μm force maps consisting of 256 force curves each were taken for each clot, with 3 clots measured per group. Mean elastic modulus ± standard deviation is reported for each group.

Assessment of fibroblast migration in an in vitro model of hemophilic wound healing

Neonatal human dermal fibroblasts (HDFn) (Gibco, Waltham, MA, USA) P8-P13 were seeded into collagen/fibrinogen matrices in a three-dimensional *in vitro* wound healing model adapted from Chen *et al* [41]. In this model, a 300 μl matrix comprising 3 mg/ml bovine collagen type I (PureCol™ EZ Gel solution, Sigma-Aldritch), 1 mg/ml human fibrinogen (FIB 3, Enzyme Research Laboratories, South Bend, IN, USA), and a 1:3000 dilution of Innovin (Dade Behring Gmbh, Marburg, GER) were seeded with 2×10^5 HDFns in a 48-well tissue culture plate (CELLTREAT Scientific Products, Pepperell, MA, USA) and polymerized for 24 hours at 37 °C. Following polymerization, a defect was made in the center of each matrix using a 2 mm biopsy punch (VWR, Radnor, PA, USA) attached to a vacuum line in order to model an injury in the matrix. Each defect was filled with 10 μl PPP clots made from either normal or hemophilia B-like plasma +/− PLPs. Clots were polymerized for two hours at 37 °C, and then the matrices and clots were covered in 300 μL HDFn growth medium (DMEM, 10% fetal bovine serum, 1% penicillin/streptomycin, 1% L-glutamine). Images were obtained immediately following induction of the defect and then every 24 hours for the next three days to visualize cell migration into the defect area from the surrounding matrix. Cell infiltration into the defect area were obtained using ImageJ by blinding images by clot group and randomly placing four 300 × 300 px squares within the defect area of each image. Cell counts within the representative squares were obtained using the ImageJ cell counter. A minimum of three samples were quantified per group per experiment, and three independent experiments were performed. Average cell count in the representative area ± standard deviation is reported for each group.

Evaluation of PLP-mediated matrix structure and fibroblast migration in the presence of platelets

In order to evaluate the impact of PLPs on fibrin deficiencies in which platelets are still present and active, 30 μL PRP clots were imaged using confocal microscopy as described above for PPP clots. Three clots were imaged per group, with three randomly placed images taken per clot. Mean clot density ± standard deviation is reported for each group. To assess the impact of platelet presence on fibroblast migration within this model, the *in vitro* fibroblast migration assay was also repeated as described previously, using PRP rather than PPP. A minimum of four samples were quantified per group per experiment, and three

independent experiments were performed. Average cell count in the representative area ± standard deviation is reported for each group.

Statistical Analysis

Statistical analysis was performed using GraphPad Prism 8 (GraphPad, San Diego, CA, USA). A ROUT outlier test (Q = 1%) was performed on all data prior to analysis; no outliers were identified. Micropost force generation results were analyzed using a non-parametric Kruskal-Wallis test with a Dunn's post-doc using a 95% confidence interval. All other results were analyzed using a Welch's ANOVA with a Games-Howell post hoc test using a 95% confidence interval.

Results and Discussion

The overarching goal of these studies was to examine the efficacy of synthetic PLPs in augmenting clotting and cell migration responses within *in vitro* models of wound healing under conditions of deficient fibrin network structure. Many strategies for augmenting clotting have been investigated in recent years, including transfusion of clotting factors and incorporation of divalent ions such as zinc; however, transfusion of clotting factors can have potentially dangerous side effects, including inhibitor development, and the impact of divalent ions on clot structure and clotting factor activity is variable and may result in both inhibitory and facilitative responses with the coagulation cascade [42, 43]. Therefore, alternatives to these potentially risky strategies are necessary in order to improve clotting and healing outcomes in patients suffering from deficient clot formation. Although many factors can influence clot formation, PLPs are able to not only augment clot formation, but also promote clot retraction, which is an important step in facilitating subsequent stages of the wound healing process, making them a potentially useful tool for improving clotting and healing outcomes in these clinical cases. However, while these PLPs have previously been shown to improve blood loss and wound healing responses in healthy systems [20, 33], their effects on fibrin structure and cell migration responses in conditions where fibrin network structure is deficient have not been thoroughly evaluated. In the studies described herein, we develop an *in vitro* model of hemophilia B using platelet-poor plasma, in which a lack of coagulation factor IX impairs the formation of robust fibrin clot networks. We then applied fibrin-targeting PLPs within these hemophilia B-like clot networks and assessed their ability to augment clot network properties and to support fibroblast migration within an *in vitro* model of wound healing. To further improve the physiological relevance of our *in vitro* models, we also investigated PLP impact on clot structure and fibroblast migration in the presence of platelets through the use of platelet-rich plasma. The results of these studies indicate that, within hemophilia-like structurally deficient fibrin networks, PLPs are able to improve clot density, clot stiffness, intra-network force generation, and fibroblast migration within a provisional clot matrix in our *in vitro* wound healing model. When applied in the presence of native platelets, PLPs were likewise able to support enhanced clot structure and fibroblast migration within these models of hemophilia-like clot network deficiency.

ULCs mimic spreading behavior of activated platelets

ULC microgels (ULCs) synthesized via precipitation polymerization of NIPAm and AAc were expected to have similar size and spreading behaviors as native activated platelets. Our previous studies have shown that ULCs formed from this reaction approximate platelet size and morphology and exhibit high deformability, as indicated by their ability to spread extensively upon glass surfaces [20, 33]. This microgel deformability, along with high fibrin affinity, is critical to PLPs' abilities to increase fibrin network density overtime through their clot retraction-mimetic actions. ULCs measured in 10 mM HEPES buffer, pH 7.4, using DLS were found to have a hydrodynamic diameter of 1.22 ± 0.11 μm. As expected, when measured on a glass surface, ULCs flattened to a height of 27 ± 22 nm (Figure 1b); this is in contrast to highly crosslinked particles of similar hydrodynamic diameter that are less deformable and have approximate heights of 117 nm when analyzed under similar conditions [34]. ULC hydrodynamic diameter is comparable in size to that of native platelets, which range from 2–5 μm in diameter [44]. Additionally, AFM measurements of ULC stiffness have determined that they exhibit modulus values of approximately 10 kPa [28] – comparable to previously determined modulus values of platelets, which range from 1–50 kPa when measured using AFM [45]. Additionally, cryogenic scanning electron microscopy images of ULCs in suspension have demonstrated that ULCs take on a morphology comparable to that of active platelets [33].

PLPs alone do not promote thrombin generation

PLPs have previously been shown to bind fibrin fibers and enhance clot formation in the presence of active fibrin polymerization [20]. The effects of PLPs on fibrin clot structure are presumably dominated via mechanical effects, i.e. crosslinking of fibrin fibers by the PLPs and subsequent induction of increased fibrin density over time, however, the influence of native platelets on fibrin formation is also due to their ability to generate thrombin on their surface. Upon initiation of the coagulation cascade, native platelets also augment fibrin formation via thrombin generation on their surfaces due to exposure of negatively charged phosphatidylserine molecules. To determine if the contribution of PLPs on fibrin structure is likewise due in part to thrombin generation, we evaluated thrombin generation in the presence of PLPs in platelet poor plasma. In thrombin generation assays, negatively charged lipids can be used in place of platelets to serve as a procoagulant surface for thrombin generation. For thrombin generation assays, plasma was incubated with tissue factor and either lipids or PLPs; thrombin generation was then measured indirectly based on the fluorescence of the samples after incubation. Lipids served as a positive control, with thrombin generation increasing as lipid concentration increases. Incorporation of PLPs into plasma resulted in curves similar to that seen for the negative plasma-only control (Figure 2), indicating that PLPs are not inherently thrombogenic and require the presence of fibrin to induce clotting. Therefore, it is likely that any effect PLPs have on clot structure and subsequent wound healing responses arises due to the fibrin specificity and high deformability of the PLPs, as these features allow the PLPs to bind within and mechanically deform clots in a manner reminiscent of the actin and myosin-driven clot retraction found in native platelets. This observed lack of innate thrombogenicity is desirable in our PLPs, as inherent thrombogenicity would be a considerable safety concern when applying PLPs *in vivo*.

Clot structure in a model of deficient fibrin formation is enhanced in the presence of PLPs

We have previously shown in purified fibrin clots that PLP-mediated retraction is due to both the high degree of deformability of the particles and high fibrin affinity of the attached fibrin antibody, allowing PLPs to bind fibrin fibers and facilitate clot retraction [33]. In these previously published studies, PLPs have been shown to bind fibrin fibers and exert strain upon bound fibers to induce clot retraction, thus stiffening clot matrices and enhancing clot structural and mechanical properties in healthy models of wound healing [33]. The PLP-mediated clot retraction occurs via a Brownian wrench mechanism, in which PLPs that have spread between bound fibers return to a more collapsed, spherical shape, and in doing so, pull the bound fibers with them to create microcollapses in the fibrin network. This initially results in both dense and highly porous areas of the clot network as fibers get pulled together, leaving empty, porous spaces; however, as this process progresses, PLP-induced microcollapses build throughout the network to ultimately bring about clot retraction. Therefore, we hypothesized that application of PLPs to clot networks with deficient fibrin structure (i.e. hemophilic) would similarly result in increased clot density and more robust network formation relative to clots with deficient fibrin structure formed in the absence of PLPs. The ability of PLPs to bind fibrin was confirmed via a preliminary fibrin-binding ELISA (Figure S1). Upon confirming the fibrin-binding capabilities of PLPs, plasma clots were formed and imaged using confocal microscopy. Confocal microscopy of clots formed from hemophilia B-like platelet poor plasma revealed that clot density is significantly increased ($p < 0.01$) under this condition of fibrin structural defect when PLPs are incorporated into the clot network (Figure 3), with clot density values approaching those seen in normal clots. We also evaluated how varying PLP concentration influenced clot structure of both normal and hemophilia clots. The increased clot density in the presence of PLPs (Figure 3) in plasma-based clots formed under conditions mimicking a hemophilia B-like fibrin structural defect is indicative of clot retraction. Indeed, under conditions of hemophilia-like conditions, the addition of PLPs into the clot resulted in an average density similar to normal conditions, despite the differences in fibrillar structure that can be observed in the confocal images of these two groups. As expected, the fibers in the hemophilia group are thicker and form a more porous network than the fibers formed in a healthy fibrin network; however, the mechanical impact of PLPs on clot structure decreases the porosity relative to that observed in the untreated hemophilia-like clot and allows for a more stable clot structure to form from these thick fibers. While the fibers of the hemophilia-like clots are thicker than those present in healthy clots, the incorporation of PLPs results in similar density values to a healthy clot containing thinner fibers with a less porous network structure.

Analysis of confocal microscopy images of clots formed from PPP at 0.25, 0.5, or 1.0 mg/ml PLP concentrations did not reveal significant differences in clot network density (Figure S2), indicating that at these concentrations, PLPs do not seem to have a dose-dependent impact on clot structure.

Cryogenic scanning electron microscopy (cryoSEM) was also used as a secondary method for analyzing clot structure. CryoSEM of PPP clots likewise revealed that clots formed in the presence of PLPs exhibited increased intersection density and decreased porosity for

haemophilia-like conditions (Figure S3). In the case of hemophilia-like clots, the addition of PLPs to the clot matrix resulted in no significant differences between the clot structure of hemophilia-like clots and normal, healthy clots, indicating that the presence of PLPs allows for recapitulation of healthy clot structure under hemophilic conditions of fibrin structural abnormalities. CryoSEM results of hemophilia-like clots formed in the absence of PLPs additionally showed heterogeneous clot structure across samples, with some hemophilia-like clots forming loose fibrin network structures and some showing very little, if any, network formation (Figure S3B). This heterogeneity within hemophilia-like clot structures reflects the established heterogeneity of naturally occurring hemophilic clots [3]. DiameterJ analysis obtained using cryoSEM images of normal and hemophilia-like plasma containing PLPs revealed increased clot density and decreased clot porosity in the presence of PLPs relative to PLP-free controls; furthermore, the addition of PLPs into hemophilia-like clots resulted in porosity and intersection density values on par with those seen in normal conditions +/− PLPs, despite the heterogeneity in clot structure observed in hemophilia-like clots. Overall, these results indicate that PLPs are able to induce clot retraction under this condition of abnormal network formation to a degree that allows for recapitulation of a healthy degree of clot network density. An important consideration in this mechanism is the length of time in which PLPs are able to bind fibrin, as this would affect PLP-mediated clot augmentation as well as clot degradation; as such, future works will investigate the time course of PLP-fibrin binding in order to better understand how this might impact clot formation and degradation kinetics.

Force generation within models of deficient fibrin clot formation is increased in the presence of PLPs

We next characterized force generation within fibrin clots using a micropost deflection method. Native platelets generate forces via actin-myosin machinery upon binding fibrin fibers within a clot; this force generation causes microcollapses in the clot network and results in increased clot density and stiffness [46]. Due to the increase in clot density observed via microscopy studies and results from our previous studies that indicate that PLPs can similarly generate forces within clot matrices, we hypothesized that PLPs would generate forces within a structurally deficient hemophilic fibrin clot network to bring about rearrangement of the fibrin network and induce clot retraction. Indeed, measurements obtained from a micropost deflection model indicated that force measurements in PLP-incorporated hemophilia-like clots was significantly higher ($p < 0.05$) relative to forces measured in standard hemophilia-like clots (Figure 4).

Results of hemophilia B-like clots containing PLPs showed two distinct populations of quantified forces; we postulate that this could have occurred due to the mechanism by which PLPs contract the clot network. As described previously, when PLPs contract a fibrin network, they exert strain upon bound fibrin fibers to induce microcollapses in the network structure. PLP-mediated clot collapse proceeds in this manner via a zipper-like Brownian wrench mechanism, which results in areas of both dense and loose fibrin networks throughout the clot prior to the achievement of total clot contraction (Figure 1d). This results in an initially heterogeneous clot structure, which could be reflected in the heterogeneous force distribution obtained from the micropost deflection model. These two populations may

also be observed due to an inherent limitation in the micropost model itself. Due to the nature of the micropost model design, force generation is calculated from the change in post-to-post distance; however, if the PLP-mediated "zipper-like" microcollapses in the network are not occurring in line with the direction in which the posts can bend towards each other, low changes in post-to-post distance may be observed. In this case, the quantified force generation would likewise be low in these samples, resulting in the second, lower population of quantified forces observed both normal + PLP and hemophilia + PLP groups in Figure 4b. Plasma itself contains inherent variability, which could also play a role in the large distributions of data observed in both PLP groups. However, as seen in Figure 4, the mean forces generated within hemophilia-like networks + PLPs allow recapitulation of forces generated within normal, healthy PLP-laden clots, indicating that the presence of PLPs in hemophilia B-like clots increases force generation within these clot networks despite the potential limitations brought about by the micropost design or the innate heterogeneity of hemophilic clots.

Due to the pNIPAM-*co*-AAc microgel composition, we expect that there may also be some residual charge effects from the AAc groups on the microgel bodies. While it is possible that this may impact PLP-fibrin interactions and dynamics, we have previously investigated the potential for these charge-based interactions to bring about force generation by examining the effect of incorporating uncoupled pNIPAM-*co*-AAc ULCs within fibrin networks [33]. No significant forces were generated in the presence of these uncoupled control particles, indicating that effects from charge interactions on PLP-mediated force generation are likely not playing a significant role in this phenomenon.

Clots with deficient fibrin formation exhibit increased stiffness in the presence of PLPs

In addition to bringing about increased network density and generating forces within fibrin networks during the process of clot retraction, native platelets also increase clot stiffness. We have previously observed that PLP-containing clots formed from purified fibrinogen polymerized with the addition of exogenous thrombin are stiffer than control clots [33]. Based on these observations, we postulated that PLPs would increase matrix stiffness when incorporated into hemophilia-like clots that exhibit structural deficiencies in their fibrin networks. AFM results obtained from force mapping of hemophilia-like and normal clots in the presence and absence of PLPs revealed that the elastic moduli of hemophilia-like clots increased significantly in the presence of PLPs relative to normal ($p < 0.01$), normal + PLP ($p < 0.05$) and hemophilia-like ($p < 0.01$) conditions (Figure 5). The stiffness of normal PPP clots was also significantly increased in the presence of PLPs relative to control normal PPP clots ($p < 0.01$).

As in the case of the micropost deflection model, force mapping of normal and hemophilia-like clots revealed a significant increase in elastic moduli of hemophilia + PLP clots relative to controls, although a wide distribution of values is likewise observed in these measurements. We again postulate that this is likely due to a combination of the inherent heterogeneity of hemophilic fibrin network structure and the Brownian wrench mechanism by which PLPs induce clot contraction; since hemophilia-like clot networks are highly porous, PLPs incorporated into these networks have more room to spread and collapse than

they do in normal clots, which could increase the effect of these network microcollapses on the overall stiffness of the clot. This, combined with the heterogeneity of hemophilic clot structure, could result in the wide modulus distribution and relatively higher stiffness values seen in the hemophilia + PLP clots relative to normal clots (+/− PLPs).

Confocal microscopy and AFM were utilized here to characterize clot density and stiffness. Additional characterization of clot strength using thromboelastography (TEG) would provide useful clinically relevant measures of hemophilic clot strength in the presence of PLPs and thus will be utilized and investigated in future works.

Cell migration is enhanced in the presence of PLPs within an in vitro model of deficient clot formation

The observed increases in clot density and accompanying increases in intra-clot force generation and stiffness led to investigations into how these structural and mechanical changes in the fibrin network would influence subsequent wound healing responses. Due to the results of numerous studies that have indicated that matrix stiffness impacts cell migration [47–49], we posited that the hemophilia-like clots containing PLPs would better facilitate fibroblast migration in an *in vitro* hemophilic wound healing model than hemophilia-like clots would alone due to the increased stiffness observed in PLP-laden hemophilia B-like clots. We investigated this by seeding dermal fibroblasts within a three-dimensional collagen/fibrinogen matrix, inducing an “injury” into the matrix via a biopsy punch, filling the “injury” defect with healthy or hemophilia-like PPP clots in the presence or absence of PLPs, and observing cell migration into the defect area over time to model the role of fibroblasts in early wound healing (post-wounding and inflammation, but before new tissue formation or tissue remodeling). Polymerization of the clots occurred via recalcification of the plasma and via the tissue factor present in the collagen/fibrinogen matrix, which allowed for a more physiologically relevant coagulation cascade to be implemented into this model. Quantification of cell migration into the defect area revealed that migration was significantly increased in the presence of PLPs under both normal ($p < 0.05$) and hemophilia-like ($p < 0.0001$) conditions relative to the no treatment conditions; furthermore, cell migration under hemophilia B-like conditions in the presence of PLPs showed no statistically significant differences in cell migration compared to healthy conditions in the presence of PLPs ($p = 0.83$), indicating that the incorporation of PLPs into hemophilia B-like clot matrices allows for recapitulation of normal cell migration behaviors in this model of *in vitro* hemophilic cell migration (Figure 6).

Average cell counts obtained from random representative areas of blinded *in vitro* wound model images demonstrated that the presence of PLPs within clot matrices enhanced fibroblast migration *in vitro* in models of both healthy (normal) and hemophilia B-like conditions; additionally, no significant difference was observed between fibroblast migration within normal and hemophilia-like clots both containing PLPs, indicating that incorporation of PLPs into hemophilia B-like clots allows the clot to act as a provisional matrix supporting cellular infiltration in a manner similar to that seen under healthy wound healing conditions. These effects were observed despite the previously observed heterogeneity in force generation within hemophilia-like clots, indicating that even the heterogeneous increase in

PLP-mediated force generation was sufficient to bring about increased matrix stiffness and fibroblast migration. In addition to an increased matrix stiffness, the PLP-containing hemophilia-like clots exhibited increased matrix density and decreased pore size compared to untreated hemophilia-like clots, providing a more favorable structure to support migration, which likely also contributed to the observed increased in migration. An important limitation that must be considered when drawing conclusions from this data is that we do not distinguish between migration and proliferation; however, initial controlling of the defect size may limit variability across groups in fibroblast proliferation that may arise due to sensation of free space. Further experimentation to better understand the migration vs. proliferation processes that are occurring within this model will be conducted in future studies and will allow for more conclusive determination of the cellular processes that may be affected by incorporation of PLPs within normal and hemophilic clot matrices.

Clot density and fibroblast migration are enhanced in the presence of PLPs within a platelet-rich environment

While the experiments previously outlined in this study were all performed using platelet-poor plasma to determine the ability of PLPs alone to enhance clotting and cell migration responses without the presence of native platelets, under *in vivo* conditions, native platelets would provide additional contractile forces to induce the retraction of a fibrin clot matrix. In some cases of fibrin structural defects, platelets can become depleted; however, in other cases, including hemophilia, platelet levels may be within normal range. Therefore, to test the influence of PLPs on clot structure and *in vitro* fibroblast migration in the presence of platelets, we analyzed responses in clots formed from platelet-rich plasma (PRP) rather than platelet-poor plasma.

Confocal microscopy of clots formed from recalcified PRP revealed that the addition of PLPs significantly increased clot density within structurally deficient hemophilia-like clots relative to hemophilia clots formed in the absence of PLPs ($p < 0.01$) (Figure 7). However, structural differences are apparent between these clots and the PPP clots imaged previously. Whereas the PPP clots displayed network structures with thicker and longer fibers, the PRP clots instead display dense centers with several thin fibers attached. This is likely due to the platelets pulling on the fibrin fibers via their actin-myosin contractile mechanism and the dense clusters we observed in these images are presumably areas in which platelet-induced microcollapses have occurred throughout the clot network. Although these dense centers are visible in all PRP conditions, the overall density of the clots formed is noticeably higher in the hemophilia + PLP group relative to the hemophilia group in the absence of PLPs, indicating that PLPs presence augments clot network structure even in the presence of native platelets. It should be noted that there were no significant differences in clot density observed under normal clotting conditions ± PLPs in the presence of platelets, but it is likely that any differences in clot formation are occurring early and are thus no longer discernable in the confocal images obtained 16 hours after initial clot formation. It is also possible that the effect of adding PLPs under this condition are less pronounced than in the hemophilia-like condition due to the vastly greater force exerted by native platelets within a clot matrix relative to those exerted by PLPs [33, 46]. Nonetheless, in our previous studies investigating the role of PLPs on wound healing outcomes *in vivo* in a rodent full thickness dermal, we

observed significant enhancement when PLPs were applied to the wound, even though this was a healthy model [33, 50] with functional platelets, which is likely due to the early influence that PLPs have on network. In these experiments, we found PLPs did not significantly increase clot density in the presence of platelets under normal, healthy conditions; this is likely due to the fact that native platelets act on a faster time scale than PLPs do within fibrin networks [33, 46]. Because of the robust fibrin formation under normal conditions, it is expected that native platelets would exert their action prior to the PLPs and are thus the primary driving force behind clot network contraction in these healthy cases. Despite the increased physiological relevance of performing these studies in the presence of platelets, the physiological relevance of this model is still limited by the absence of other blood components, such as erythrocytes, which have an effect on clot structure and mechanics in native clotting. Although the purpose of these studies was to observe PLP effects within simplified *in vitro* models of hemophilic coagulation, observing PLP effects within whole blood (both normal and hemophilic) will be necessary to better understand PLP efficacy in enhancing clot structure within a physiologically relevant environment.

We next evaluated fibroblast migration through platelet rich clots in the presence or absence of PLPs. Incorporation of recalcified PRP clots into the *in vitro* fibroblast migration model revealed enhanced fibroblast migration into hemophilia-like clots containing PLPs relative to control hemophilia-like clots ($p < 0.05$) three days after initial injury (Figure 8). Furthermore, in this *in vitro* model, the presence of PLPs within the structurally deficient hemophilia-like clots allowed for fibroblast migration on par with that seen in normal PRP clots that do not contain structural abnormalities within their fibrin networks ($p = 0.35$). As in the confocal microscopy results of PRP clots, we again did not observe significant differences between fibroblast migration in the presence or absence of PLPs under normal conditions, despite the differences observed in hemophilic clots in the presence of PLPs. We posit again that this is likely tied to the greater contractile forces exerted by platelets within a fibrin network in comparison to PLPs within a fibrin network. Estimates of force exerted by a single platelet have been found to be between 1.5 and 79 nN [46], whereas force exerted by a single PLP has been found to be approximately 6 pN [33]. It should be noted that while these results indicate that *in vitro* fibroblast migration responses are improved in platelet-rich hemophilic plasma clots in the presence of PLPs, there are additional considerations that must be taken into account when assessing PLP efficacy within physiologically relevant models; one significant consideration is the effect of PLPs on other blood cells. Studies into the hemolysis ratio of the PLPs when incubated with whole blood would provide critical information as to the safety of applying these particles within more complex physiological systems, both *in vitro* and *in vivo*, prior to drawing conclusions as to the overall safety and efficacy of applying PLPs to hemophilic clot networks within these systems.

An additional consideration for translation of PLPs to clinical use is gaining a robust understanding of *in vivo* fate of the particles. Previous studies have shown that, when incorporated into *in vivo* wounds, PLPs incorporate with native fibrin forming at wound sites [33]. In a separate set of studies investigating nanosilver composite PLPs in an infected wound model, we did not observe particles in histological sections 9 days post-injury [50], indicating that PLPs are cleared when applied topically; however, detailed studies into the eventual clearance mechanism of PLPs in this application have not yet been performed.

Therefore, in addition to the aforementioned hemolysis studies, evaluation of the clearance mechanism of these particles after application to external wounds is a key future experiment that will allow better understanding of the potential that PLPs may hold for improving clinical treatments for patients suffering from conditions involving dysfunctional clotting, such as hemophilia.

Conclusions

Overall, these studies show that our synthetic PLPs are capable of interacting with structurally deficient fibrin clot networks to enhance clot structure, generate forces within clot matrices, increase matrix stiffness, and promote cell migration under conditions of abnormal network and fibrillar structure. These findings support our overarching hypothesis that PLP-mediated clot retraction leads to increased matrix stiffness that facilitates enhanced cell migration. Previous studies performed under normal clot formation conditions indicated that PLP-mediated clot contraction plays an important role in wound healing through the promotion of fibroblast migration into the wound site, allowing for subsequent matrix repair and remodeling [33]. However, in many clinical coagulation cases, fibrin clot formation is disrupted or dysfunctional; therefore, evaluation of fibrin-binding PLPs within a model of deficient fibrin clot formation was necessary to gain a better understanding of the translational potential of PLPs. The ability of PLPs to augment clot stability and facilitate cell migration into structurally deficient clot networks *in vitro* as demonstrated in fibroblast migration experiments indicates that application of PLPs could also provide a biomimetic material for improving overall wound healing events in models of diseases that result in deficient clot formation, such as hemophilia or von Willebrand's disease, or with antithrombotic therapies that interfere with clot formation [15–17]. Patients with such conditions could greatly benefit from adjunct therapy strategies to enhance current treatment modalities, and PLPs could address these limitations of current therapies.

Furthermore, artificial cell constructs made from synthetic materials pose an intriguing option for developing a hemostatic technology capable of augmenting clotting and improving healing outcomes without generating the risk of inhibitor development associated with clotting factor treatments. Synthetic material-based strategies can be advantageous alternatives to purely biological treatments due to their relatively low cost of manufacturing and ease of tunability, which allows for the recapitulation of desired biological functions via surface modifications and/or changes in material properties. Indeed, the PLPs described in these works are easily manufactured and have been shown to possess desirable size, mechanical properties, and fibrin-binding abilities that allow them to mimic the hemostatic and clot retraction abilities of native platelets. Critical future works are necessary to further evaluate the translational potential of PLPs for treatment of hemophilia and/or other conditions involving deficient clot formation; evaluation of PLP safety *in vitro* and *in vivo* through hemolysis and clearance studies, as well as animal models of hemophilic wound healing in the presence of PLPs, will be important next steps in evaluating the efficacy of this technology.

Supplementary Material

Refer to Web version on PubMed Central for supplementary material.

Acknowledgements

Funding for this project was provided by the American Heart Association (16SDG29870005) and (18PRE33990338) to EM, the National Institutes of Health NIAMS (R21AR071017), the National Science Foundation CAREER DMR (1847488), and the National Institutes of Health NCATS (UL1TR001117). This work was performed in part at the North Carolina State University Analytical Instrumentation Facility (AIF), which is supported by the State of North Carolina and the National Science Foundation (ECCS-1542015). The AIF is part of the North Carolina Research Triangle Nanotechnology Network (RTNN), a site in the National Nanotechnology Coordinated Infrastructure (NNCI). The authors acknowledge Chuanzhen Zhou at the AIF for assistance with cryoSEM, Eva Johannes at the CMIF for assistance with confocal microscopy, and Dr. Michael Daniele and Dr. Patrick Erb for assistance with micropost mold design and fabrication.

Abbreviations

PLP	platelet-like particle

References

[1]. Geddis AE, The regulation of proplatelet production, Haematologica 94(6) (2009) 756–759. [PubMed: 19483152]

[2]. Modery-Pawlowski CL, Tian LL, Pan V, McCrae KR, Mitragotri S, Sen Gupta A, Approaches to synthetic platelet analogs, Biomaterials 34(2) (2013) 526–541. [PubMed: 23092864]

[3]. Monroe DM, Hoffman M, What Does It Take to Make the Perfect Clot?, Arteriosclerosis, Thrombosis, and Vascular Biology 26(1) (2006) 41.

[4]. Nandi S, Brown AC, Platelet-mimetic strategies for modulating the wound environment and inflammatory responses, Exp Biol Med (Maywood) 241(10) (2016) 1138–1148. [PubMed: 27190260]

[5]. Cines DB, Lebedeva T, Nagaswami C, Hayes V, Massefski W, Litvinov RI, Rauova L, Lowery TJ, Weisel JW, Clot contraction: compression of erythrocytes into tightly packed polyhedra and redistribution of platelets and fibrin, Blood 123(10) (2014) 1596–1603. [PubMed: 24335500]

[6]. Kim OV, Litvinov RI, Alber MS, Weisel JW, Quantitative structural mechanobiology of platelet-driven blood clot contraction, Nat Commun 8 (2017) 1274. [PubMed: 29097692]

[7]. Tutwiler V, Litvinov RI, Lozhkin AP, Peshkova AD, Lebedeva T, Ataullakhanov FI, Spiller KL, Cines DB, Weisel JW, Kinetics and mechanics of clot contraction are governed by the molecular and cellular composition of the blood, Blood 127(1) (2016) 149–159. [PubMed: 26603837]

[8]. Weisel JW, Fibrinogen and Fibrin, Advances in Protein Chemistry, Academic Press 2005, pp. 247–299.

[9]. Dickinson LE, Gerecht S, Engineered Biopolymeric Scaffolds for Chronic Wound Healing, Frontiers in Physiology 7 (2016).

[10]. Injury Prevention & Control, 2017 https://www.cdc.gov/injury/wisqars/LeadingCauses.html. (Accessed January 24 2020).

[11]. Data & Statistics on Hemophilia, 2018 https://www.cdc.gov/ncbddd/hemophilia/data.html. 2019).

[12]. Hoffman M, Harger A, Lenkowski A, Hedner U, Roberts HR, Monroe DM, Cutaneous wound healing is impaired in hemophilia B, Blood 108(9) (2006) 3053. [PubMed: 16825491]

[13]. Wolberg AS, Allen GA, Monroe DM, Hedner U, Roberts HR, Hoffman M, High dose factor VIIa improves clot structure and stability in a model of haemophilia B, British Journal of Haematology 131(5) (2005) 645–655. [PubMed: 16351642]

[14]. He S, Blombäck M, Jacobsson Ekman G, Hedner U, The role of recombinant factor VIIa (FVIIa) in fibrin structure in the absence of FVIII/FIX, Journal of Thrombosis and Haemostasis 1(6) (2003) 1215–1219. [PubMed: 12871322]

[15]. Jameson SS, Rymaszewska M, James P, Serrano-Pedraza I, Muller SD, Hui ACW, Reed MR, Wound Complications Following Rivaroxaban Administration: A Multicenter Comparison with Low-Molecular-Weight Heparins for Thromboprophylaxis in Lower Limb Arthroplasty, JBJS 94(17) (2012).

[16]. Cotton BA, McCarthy JJ, Holcomb JB, Acutely Injured Patients on Dabigatran, New England Journal of Medicine 365(21) (2011) 2039–2040. [PubMed: 22111735]

[17]. Leebeek FWG, Eikenboom JCJ, Von Willebrand's Disease, New England Journal of Medicine 375(21) (2016) 2067–2080. [PubMed: 27959741]

[18]. Doshi N, Zahr AS, Bhaskar S, Lahann J, Mitragotri S, Red blood cell-mimicking synthetic biomaterial particles, Proceedings of the National Academy of Sciences of the United States of America 106(51) (2009) 21495–21499. [PubMed: 20018694]

[19]. Hickman DA, Pawlowski CL, Shevitz A, Luc NF, Kim A, Girish A, Marks J, Ganjoo S, Huang S, Niedoba E, Sekhon UDS, Sun M, Dyer M, Neal MD, Kashyap VS, Sen Gupta A, Intravenous synthetic platelet (SynthoPlate) nanoconstructs reduce bleeding and improve 'golden hour' survival in a porcine model of traumatic arterial hemorrhage, Sci Rep 8(1) (2018) 3118. [PubMed: 29449604]

[20]. Brown AC, Stabenfeldt SE, Ahn B, Hannan RT, Dhada KS, Herman ES, Stefanelli V, Guzzetta N, Alexeev A, Lam WA, Lyon LA, Barker TH, Ultrasoft microgels displaying emergent platelet-like behaviours, Nature Materials 13(12) (2014) 1108–1114. [PubMed: 25194701]

[21]. Nayak S, Lyon LA, Soft Nanotechnology with Soft Nanoparticles, Angewandte Chemie International Edition 44(47) (2005) 7686–7708. [PubMed: 16283684]

[22]. Kobayashi J, Okano T, Design of Temperature-Responsive Polymer-Grafted Surfaces for Cell Sheet Preparation and Manipulation, Bulletin of the Chemical Society of Japan 92(4) (2019) 817–824.

[23]. Dhowre HS, Rajput S, Russell NA, Zelzer M, Responsive cell–material interfaces, Nanomedicine 10(5) (2015) 849–871. [PubMed: 25816884]

[24]. Ariga K, Jia X, Song J, Hsieh C-T, Hsu S.-h., Materials Nanoarchitectonics as Cell Regulators, ChemNanoMat 5(6) (2019) 692–702.

[25]. Merkel TJ, Jones SW, Herlihy KP, Kersey FR, Shields AR, Napier M, Luft JC, Wu H, Zamboni WC, Wang AZ, Bear JE, DeSimone JM, Using mechanobiological mimicry of red blood cells to extend circulation times of hydrogel microparticles, Proceedings of the National Academy of Sciences 108(2) (2011) 586.

[26]. Doshi N, Orje JN, Molins B, Smith JW, Mitragotri S, Ruggeri ZM, Platelet Mimetic Particles for Targeting Thrombi in Flowing Blood, Advanced Materials 24(28) (2012) 3864–3869. [PubMed: 22641451]

[27]. Bertram JP, Williams CA, Robinson R, Segal SS, Flynn NT, Lavik EB, Synthetic Platelets: Nanotechnology to Halt Bleeding, Science translational medicine 1(11) (2009) 11ra22.

[28]. Bachman H, Brown AC, Clarke KC, Dhada KS, Douglas A, Hansen CE, Herman E, Hyatt JS, Kodlekere P, Meng Z, Saxena S, Spears MW Jr, Welsch N, Lyon LA, Ultrasoft, highly deformable microgels, Soft Matter 11(10) (2015) 2018–2028. [PubMed: 25648590]

[29]. Senff H, Richtering W, Temperature sensitive microgel suspensions: Colloidal phase behavior and rheology of soft spheres, The Journal of Chemical Physics 111(4) (1999) 1705–1711.

[30]. Gao J, Frisken BJ, Cross-Linker-Free N-Isopropylacrylamide Gel Nanospheres, Langmuir 19(13) (2003) 5212–5216.

[31]. Gao J, Frisken BJ, Influence of Secondary Components on the Synthesis of Self-Cross-Linked N -Isopropylacrylamide Microgels, Langmuir 21(2) (2005) 545–551. [PubMed: 15641822]

[32]. Monroe D, Hoffman M, The clotting system - A major player in wound healing, Haemophilia 18 Suppl 5 (2012) 11–6. [PubMed: 22757679]

[33]. Nandi S, Sproul EP, Nellenbach K, Erb M, Gaffney L, Freytes DO, Brown AC, Platelet-like particles dynamically stiffen fibrin matrices and improve wound healing outcomes, Biomaterials Science 7(2) (2019) 669–682. [PubMed: 30608063]

[34]. Joshi A, Nandi S, Chester D, Brown AC, Muller M, Study of poly (N-isopropylacrilamide-co-acrylic acid) (pNIPAM) microgel particle induced deformations of tissue mimicking phantom by ultrasound stimulation, Langmuir (2017) 1457–1465.

[35]. Sproul EP, Nandi S, Roosa C, Schreck L, Brown AC, Biomimetic Microgels with Controllable Deformability Improve Healing Outcomes, Advanced Biosystems 0(0) (2018) 1800042.

[36]. Hotaling NA, Bharti K, Kriel H, Simon CG, DiameterJ: A validated open source nanofiber diameter measurement tool, Biomaterials 61 (2015) 327–338. [PubMed: 26043061]

[37]. Thavandiran N, Dubois N, Mikryukov A, Massé S, Beca B, Simmons CA, Deshpande VS, McGarry JP, Chen CS, Nanthakumar K, Keller GM, Radisic M, Zandstra PW, Design and formulation of functional pluripotent stem cell-derived cardiac microtissues, Proceedings of the National Academy of Sciences of the United States of America 110(49) (2013) E4698–E4707. [PubMed: 24255110]

[38]. Hansen A, Eder A, Bonstrup M, Flato M, Mewe M, Schaaf S, Aksehrlioglu B, Schwoerer A, Uebeler J, Eschenhagen T, Development of a drug screening platform based on engineered heart tissue., Circulation Research 107(1) (2010) 35–44. [PubMed: 20448218]

[39]. Vandenburgh H, High-Content Drug Screening with Engineered Musculoskeletal Tissues, Tissue Eng Part B Rev 16(1) (2010) 55–64. [PubMed: 19728786]

[40]. Kim TK, Kim JK, Jeong OC, Measurement of nonlinear mechanical properties of PDMS elastomer, Microelectronic Engineering 88(8) (2011) 1982–1985.

[41]. Chen Z, Yang J, Wu B, Tawil B, A Novel Three-Dimensional Wound Healing Model, Journal of Developmental Biology 2(4) (2014) 198–209.

[42]. Henderson SJ, Xia J, Wu H, Stafford AR, Leslie BA, Fredenburgh JC, Weitz DA, Weitz JI, Zinc promotes clot stability by accelerating clot formation and modifying fibrin structure, Thrombosis and haemostasis 115(3) (2016) 533–542. [PubMed: 26489782]

[43]. Inhibitors and Hemophilia.https://www.cdc.gov/ncbddd/hemophilia/inhibitors.html. 2019).

[44]. Krishnegowda M, Rajashekaraiah V, Platelet disorders: an overview, Blood Coagulation & Fibrinolysis 26(5) (2015).

[45]. Radmacher M, Fritz M, Kacher CM, Cleveland JP, Hansma PK, Measuring the viscoelastic properties of human platelets with the atomic force microscope, Biophysical journal 70(1) (1996) 556–567. [PubMed: 8770233]

[46]. Lam WA, Chaudhuri O, Crow A, Webster KD, Li T-D, Kita A, Huang J, Fletcher DA, Mechanics and contraction dynamics of single platelets and implications for clot stiffening, Nature Materials 10(1) (2011) 61–66. [PubMed: 21131961]

[47]. Barriga EH, Franze K, Charras G, Mayor R, Tissue stiffening coordinates morphogenesis by triggering collective cell migration in vivo, Nature 554(7693) (2018) 523–527. [PubMed: 29443958]

[48]. Discher DE, Janmey P, Y.-l. Wang, Tissue Cells Feel and Respond to the Stiffness of Their Substrate, Science 310(5751) (2005) 1139. [PubMed: 16293750]

[49]. Solon J, Levental I, Sengupta K, Georges PC, Janmey PA, Fibroblast Adaptation and Stiffness Matching to Soft Elastic Substrates, Biophysical Journal 93(12) (2007) 4453–4461. [PubMed: 18045965]

[50]. Chee E, Nandi S, Nellenbach K, Mihalko E, Snider DB, Morrill L, Bond A, Sproul E, Sollinger J, Cruse G, Hoffman M, Brown AC, Nanosilver composite pNIPAm microgels for the development of antimicrobial platelet-like particles, Journal of Biomedical Materials Research Part B: Applied Biomaterials n/a(n/a) (2020).

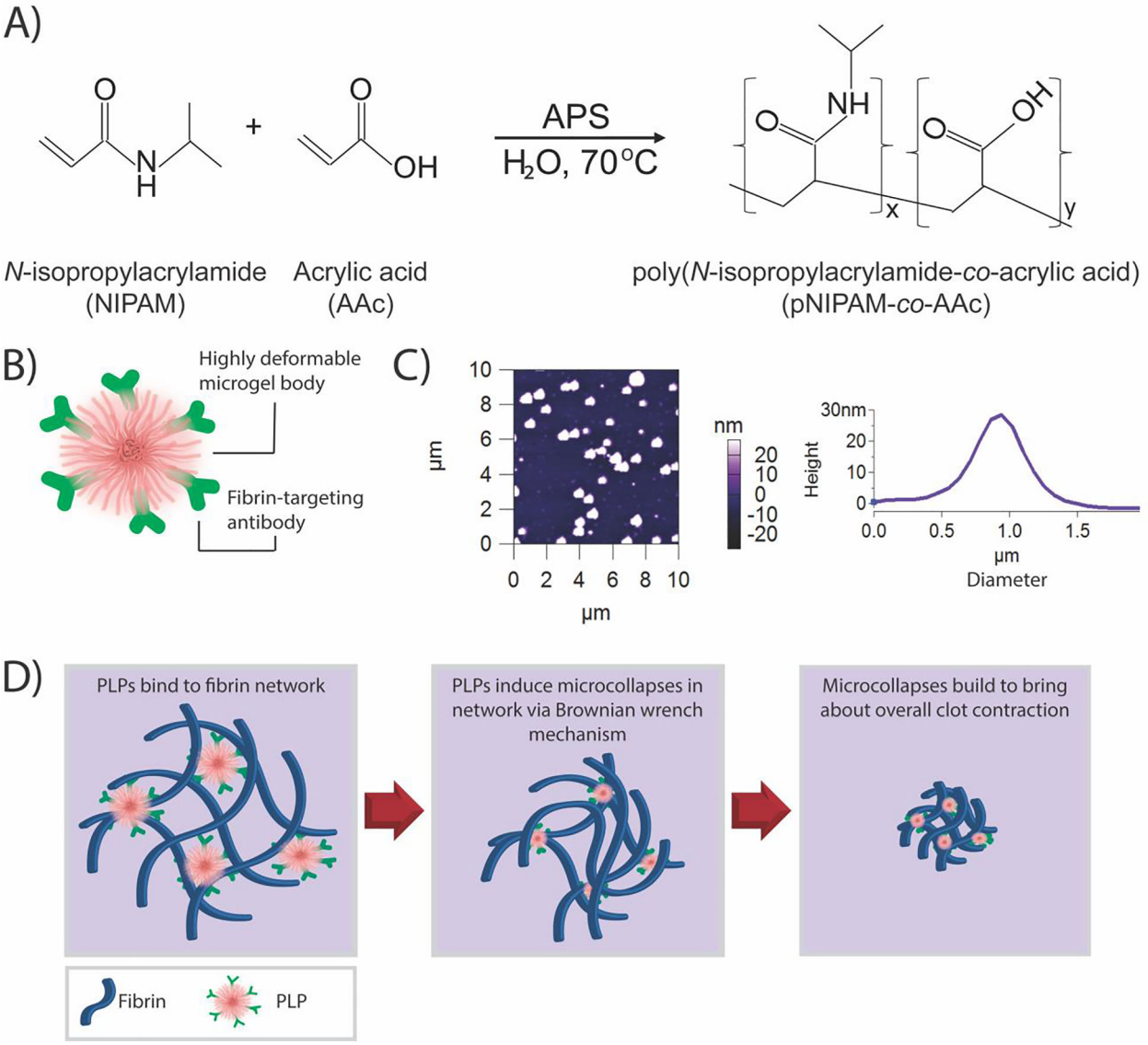

Figure 1: Overview of PLP design and clot retraction action.

A) Overview of pNIPAM-*co*-AAc ULC microgel synthesis reaction. B) PLPs are synthesized by coupling a fibrin-targeting antibody to an ultralow crosslinked highly deformable pNIPAM-*co*-AAc microgel body (ULC). C) Atomic force microscopy reveals that ULCs deform upon a glass coverslip to flatten to an average height of 27 ± 22 nm and a diameter of 1.22 ± 0.11 μm. n = 30 particles. A representative AFM scan and height trace are shown. D) Once ULCs are coupled to a fibrin-targeting antibody to form PLPs, the PLPs are able to bind fibrin fibers forming at a site of injury. PLPs become spread as they stretch between bound fibers, and then collapse inward to return to a more energetically favorable spherical conformation. When this occurs, PLPs exert strain upon the bound fibers, inducing microcollapses in the clot network that sum via a Brownian wrench mechanism to bring about bulk clot contraction.

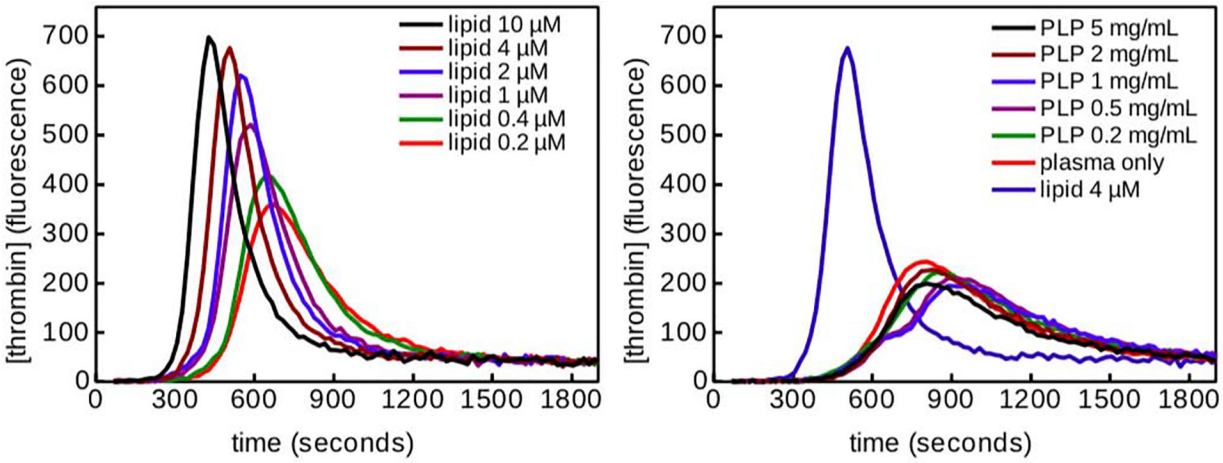

Figure 2: Thrombin generation assay demonstrates that PLPs alone are not thrombogenic.

Plasma was incubated with tissue factor and lipids (left) or PLPs (right). Thrombin generation was measured indirectly based on the fluorescence of the samples after incubation. Lipids served as a positive control, with thrombin generation increasing as lipid concentration increases. Incorporation of PLPs into plasma resulted in curves similar to that seen for the negative plasma-only control, indicating that PLPs are not inherently thrombogenic and require the presence of fibrin in order to induce clotting.

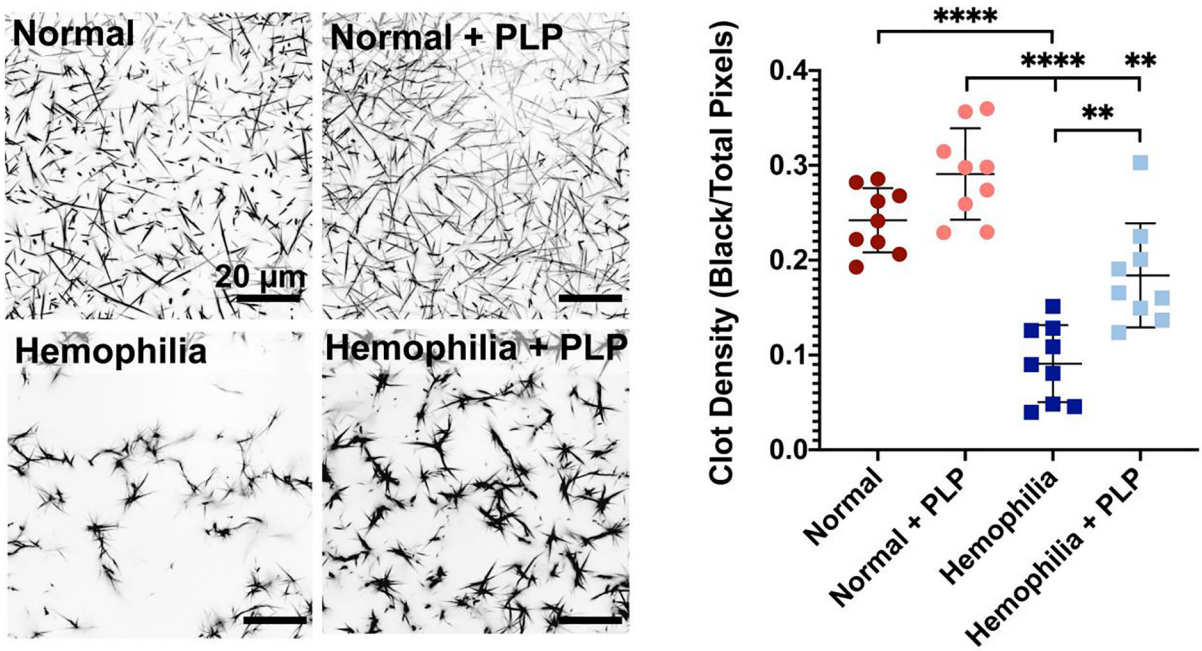

Figure 3: Clot density is significantly increased in the presence of PLPs under a haemophilia-like condition of deficient fibrin network formation.

Clots were formed from recalcified platelet poor plasma (PPP) in the absence (normal conditions) or presence of an anti-factor IX (fIX) antibody (hemophilia conditions) +/− the addition of 0.5 mg/mL PLPs. Clots were imaged using confocal microscopy 16 hours after initial clot formation. Clot density was determined using Image J and is represented as total black pixels (fibrin fibers) over total pixels present within each image. n = 3 clots/group; 3 locations imaged/clot. Plots show individual data points and mean ± standard deviation of each group. **p < 0.01; ****p < 0.0001.

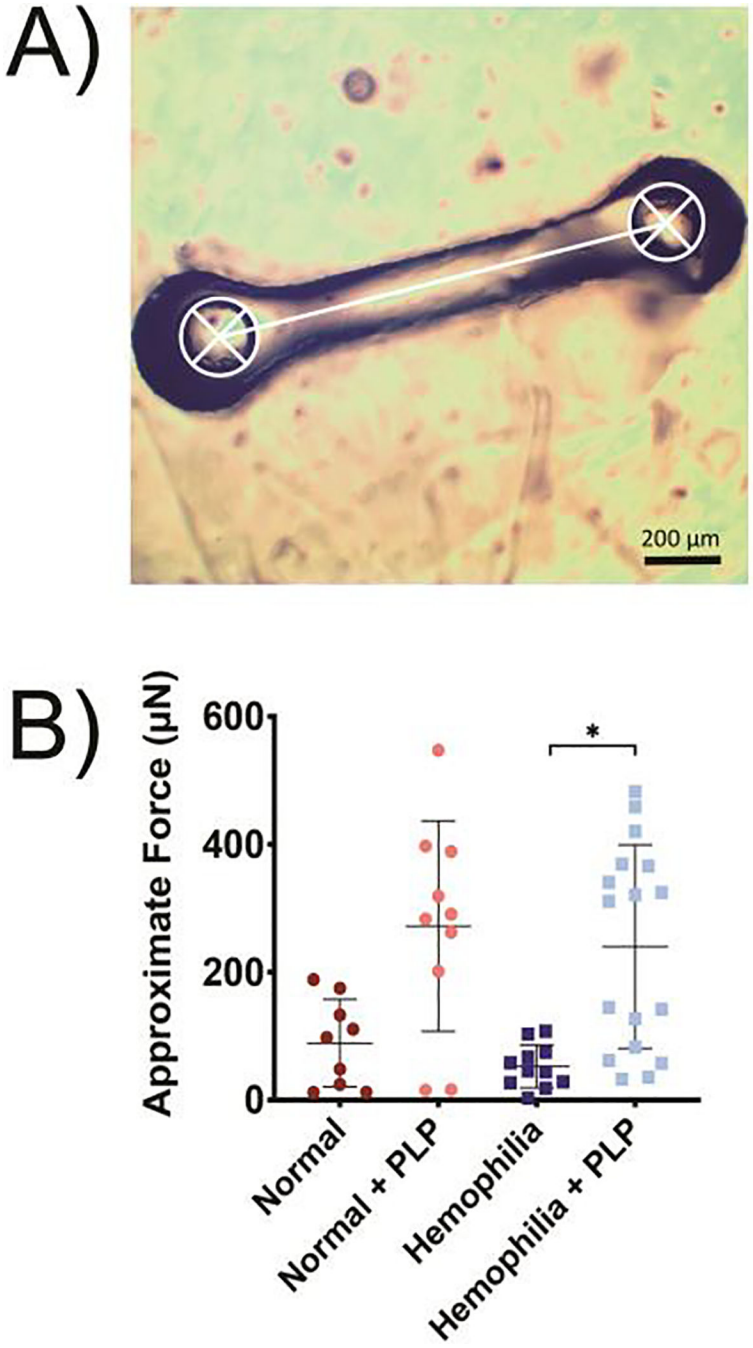

Figure 4: Forces generated within fibrin networks were quantified using a micropost deflection model.

A) Clots formed from recalcified platelet poor plasma (PPP) in the absence (normal conditions) or presence of an anti-factor IX (fIX) antibody (hemophilia conditions) +/− the addition of 0.5 mg/mL PLPs were seeded around PDMS microposts, and post-to-post distance (represented in white) was obtained using ImageJ. B) Approximate force generation within structurally deficient hemophilia fibrin networks is significantly increased in the presence of PLPs. A minimum of 9 clots were analyzed per group, and individual data points as well as means ± standard deviations are represented for each group. *$p < 0.05$.

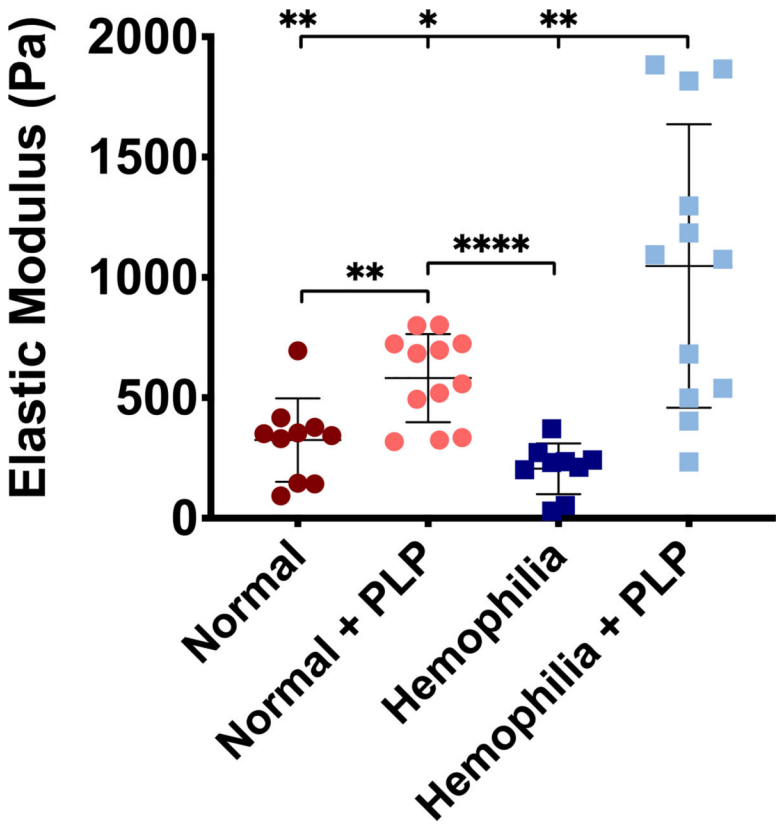

Figure 5: Atomic force microscopy nanoindentation of platelet poor plasma (PPP) clots reveals increased clot stiffness in clots incorporated with PLPs.

Clots formed from recalcified PPP in the absence (normal conditions) or presence of an anti-factor IX (fIX) antibody (hemophilia conditions) +/− the addition of 0.5 mg/mL PLPs were analyzed via AFM nanoindentation to determine clot stiffness 16 hours after initial clot polymerization. Both normal and structurally deficient hemophilia-like clots exhibit significantly greater stiffness in the presence of PLPs when compared to normal or hemophilia-like control clots, respectively. n = 3–4 clots per group; 3 locations imaged per clot; 256 forcemaps per location. Individual data and means ± standard deviations are represented for each group. *$p < 0.05$; **$p < 0.01$; ****$p < 0.0001$.

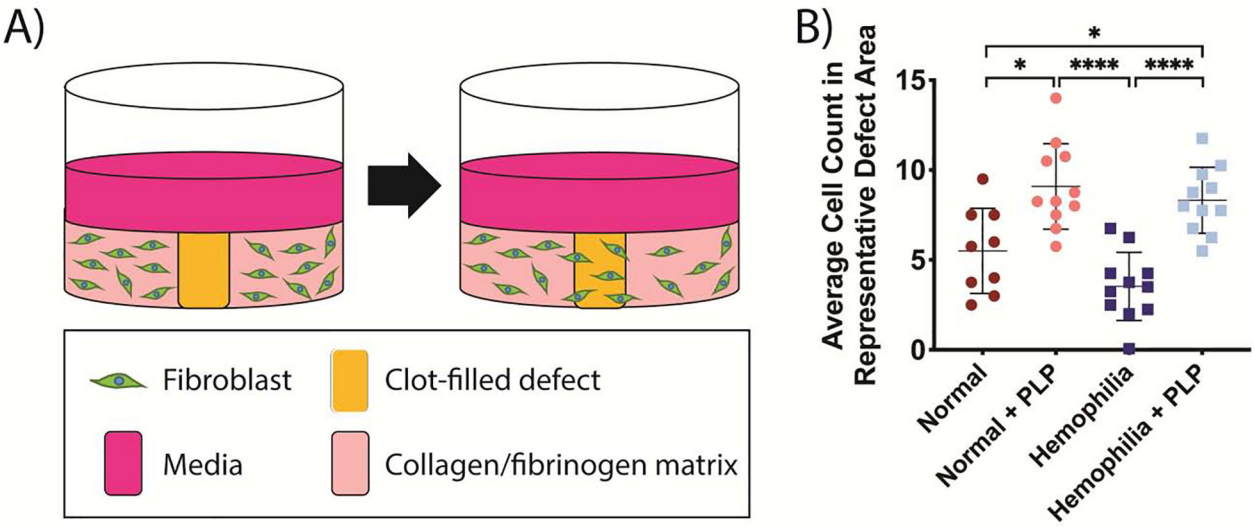

Figure 6: Analysis of cell migration in an *in vitro* injury model.

A) Schematic of *in vitro* fibroblast migration model. Fibroblasts are seeded into a collagen/fibrinogen matrix containing tissue factor, which then undergoes an "injury" via a biopsy punch. The injured area is filled with a clot formed from recalcified platelet poor plasma (PPP), and fibroblast migration into the wounded area is observed over time. B) Average fibroblast counts within representative 300 px^2 areas of images obtained 3 days after initial injury. Fibroblast migration was significantly increased into both normal and structurally deficient hemophilia-like clots in the presence of PLPs. Incorporation of PLPs into hemophilia-like clots allowed for recapitulation of fibroblast migration back to levels seen in normal PPP clots formed in the presence of PLPs. Three independent experiments were conducted, with n = 3–4 per group per experiment. Individual data points as well as means ± standard deviations are shown for each group. *$p < 0.05$; ****$p < 0.0001$.

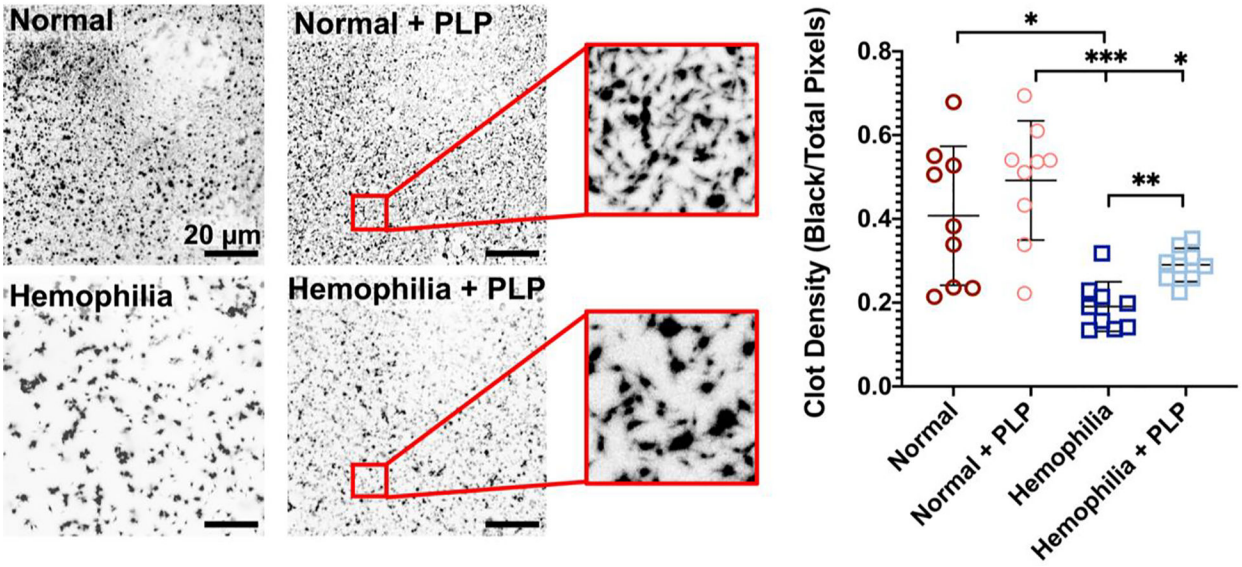

Figure 7: Confocal microscopy of clots formed from recalcified platelet rich plasma (PRP) reveals significantly enhanced clot density in structurally deficient hemophilia-like clots containing PLPs relative to control hemophilia-like clots.

Clots were formed from recalcified platelet rich plasma (PRP) in the absence (normal conditions) or presence of an anti-factor IX (fIX) antibody (hemophilia conditions) +/− the addition of 0.5 mg/mL PLPs. Clots were imaged using confocal microscopy 16 hours after initial clot formation. Clot density was determined using Image J and is represented as total black pixels (fibrin fibers) over total pixels present within each image. Clots formed from recalcified PRP display thinner fiber structure when viewed at a 5.06 μm^2 scan at 63X, and closer inspection of these clots, as seen in the area outlined in red, reveals clot structures comprising distinct thin fibers clustered around dense fibrin pockets. n = 3 clots per group; 3 locations imaged per clot. Individual data points and mean ± standard deviation are represented for each group. *$p < 0.05$; **$p < 0.01$.

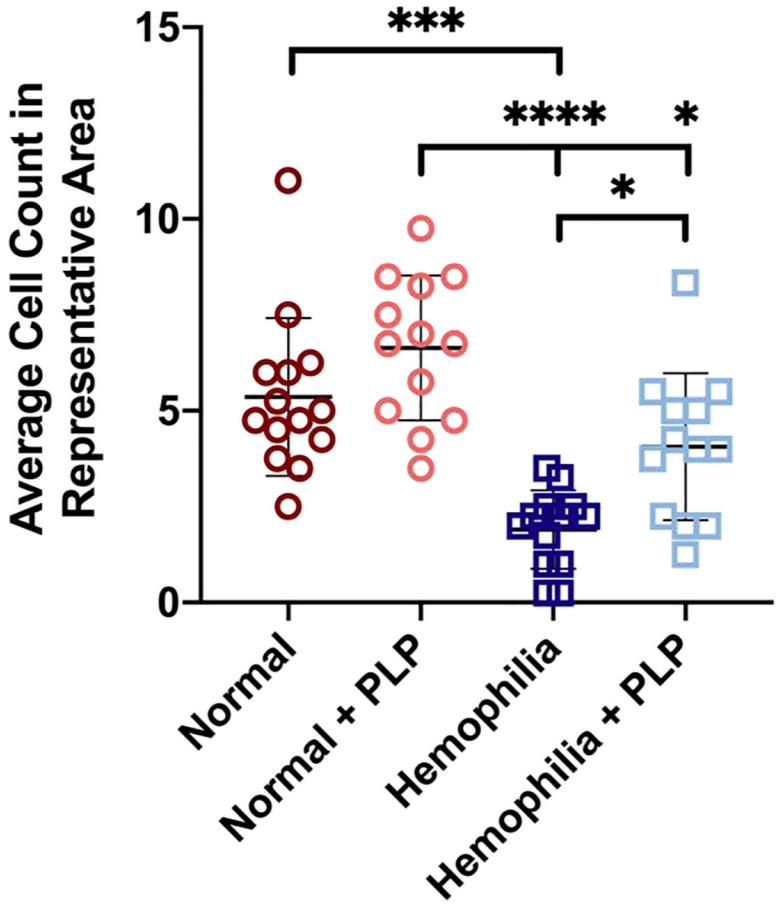

Figure 8: *In vitro* assessment of fibroblast migration within recalcified platelet rich plasma (PRP) clots.

Fibroblasts were seeded into a collagen/fibrinogen matrix containing tissue factor, which then undergoes an "injury" via a biopsy punch. The injured area is filled with a clot formed from recalcified PRP, and fibroblast migration into the wounded area is observed over time. Average fibroblast counts within representative 300 px^2 areas of images obtained 3 days after initial injury. Hemophilia-like structurally deficient PRP clots were able to support similar levels of fibroblast migration as normal clots after incorporation of PLPs and significantly greater fibroblast migration than control hemophilia-like PRP clots. Three independent experiments were conducted; n = 4–5 per group per experiment. Individual data points and mean ± standard deviation are represented for each group. *$p < 0.05$; ***$p < 0.001$; ****$p < 0.0001$.